Transmission Lines Exposed to External Electromagnetic Fields in Low Frequencies

George P. Veropoulos[a] and Panagiotis J. Papakanellos[b]

[a]*Division of Academic Studies, Hellenic Navy Petty Officers Academy, 12400 Skaramagkas, Athens, Greece*
[b]*Hellenic Air Force Academy, 1010 Dekelia, Athens, Greece*

Abstract. This paper presents a complete review of the standard transmission-line model (STL) for two-wire transmission lines exposed to external electromagnetic fields. The validity of the STL model is limited to frequency ranges where the transverse characteristic dimension of the line is electrically short. This model is derived from Maxwell's equations in terms of voltage and current at the ends of the line. We examine terminated transmission lines, which are excited by nonuniform fields. Numerical results for the induced load voltages show notable deviations from those obtained under the assumption of plane-wave incidence.

Keywords: standard transmission-line model; nonuniform electromagnetic fields; two-wire transmission line; electromagnetic compatibility.

PACS: 41.20.-q

INTRODUCTION

The electromagnetic (EM) field coupling to transmission lines has a great practical interest for many electromagnetic compatibility (EMC) studies and applications (e.g. plethora of the cables associated with most of the audio/video interfaces and host bus adapters).

The analysis of the EM field coupling to transmission lines can be performed exactly via Maxwell's equations. These equations are transformed into integral equations, which may be solved numerically by applying standard numerical techniques (like the well-known moment methods [1]). However, a systematic use of such methods becomes cumbersome due to large storage and computer time requirements.

For sufficiently low frequencies, the problem can be solved using the transmission-line approximation or standard transmission-line model (STL) [2]. The main assumptions for this approach are as follows:

a. Propagation occurs along the line axis. If the cross-sectional dimensions of the line conductors are electrically small, propagation can indeed be assumed to occur essentially along the line axis only.
b. The sum of the line currents at any cross section of the line is zero. We are concerned with transmission-line mode currents and neglecting the so-called "antenna mode" ones. This is a good approximation if we wish to compute the load response of the line, because the antenna-mode current is small near the end of line.
c. The response of the line to the coupled EM fields is quasi-transverse electromagnetic (TEM). The condition that the response of the line is quasi-TEM is satisfied only up to the cutoff frequency, above which higher-order modes begin to appear [2]. In some cases, e.g.

finite parallel plates or coaxial lines, it is possible to derive an exact expression for the cutoff frequency, below which only TEM mode exists [3].

For higher frequencies, where the STL model is not valid, many authors have proposed the extension of the STL theory to such frequency ranges through models that retain the simplicity of the STL model [4-6]. In this way, it is possible to overcome serious problems associated with full-wave numerical simulations (computational cost). In this paper, we apply the assumptions of the STL model in a two-wire transmission line. We will first derive the field-to-transmission line coupling equations following the analysis of [2, 7, 8].

DERIVATION OF THE GENERALIZED TELEGRAPHER'S EQUATIONS

We consider the case of a uniform two-wire transmission line, terminated in linear loads Z_1 and Z_2. The transmission line is defined by the geometrical parameters shown in Figure 1 (namely the wire radius α, the distance between the conductors b and the length s). The line is immersed in a lossy dielectric medium and is illuminated by an external EM field with intensities $\vec{E}^{\,\mathrm{inc}}$ and $\vec{H}^{\,\mathrm{inc}}$.

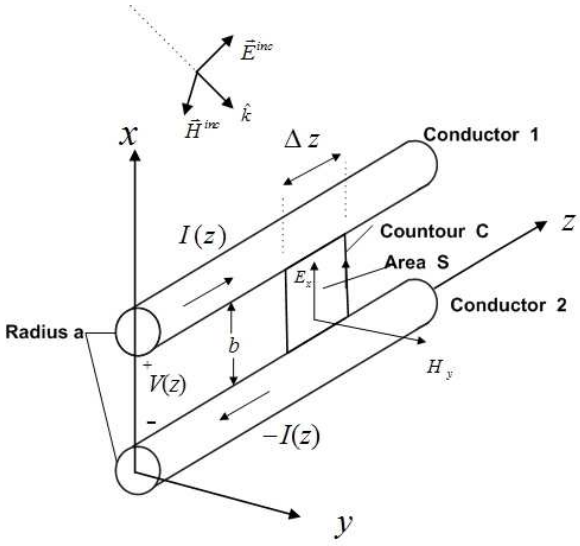

FIGURE 1. Geometry of a two-wire transmission line in an incident EM field**.**

The problem of interest is the calculation of the induced voltages at the terminations. The total fields $\vec{E}$ and $\vec{H}$ may be decomposed into two different components, the incident fields ($\vec{E}^{\,\mathrm{inc}}$ and $\vec{H}^{\,\mathrm{inc}}$), which exist in the absence of the transmission line, and the scattered fields ($\vec{E}^{\,\mathrm{sca}}$ and $\vec{H}^{\,\mathrm{sca}}$), which are generated by the currents and charges flowing on the conductors. To develop equations for the induced line currents in terms of the incident fields $\vec{E}^{\,\mathrm{inc}}$ and $\vec{H}^{\,\mathrm{inc}}$, Stokes' theorem is used. The theorem states that any vector field $\vec{F}$ satisfies

$$\int_{\mathrm{C}} \vec{F} \cdot d\vec{l} = \iint_{\mathrm{S}} \vec{\nabla} \times \vec{F} \cdot d\vec{S} \tag{1}$$

where C is a closed contour enclosing an area S, as shown in Figure 1. Letting $\vec{F}$ represent the electric field $\vec{E}$ and applying this expression to the pertinent Maxwell's equation for the time-harmonic variation of the form $e^{j\omega t}$, one obtains

$$\vec{\nabla} \times \vec{E} = -j\omega\mu_0 \vec{H} \tag{2}$$

or

$$\int_C \vec{E} \cdot d\vec{l} = -j\omega\mu_0 \iint_S \vec{H} \cdot d\vec{S} \tag{3}$$

Since the contour has a differential width Δz, (3) can be written as

$$\begin{aligned} &\int_0^b \left[E_x(x,0,z+\Delta z) - E_x(x,0,z)\right]dx - \int_z^{z+\Delta z} \left[E_z(b,0,z) - E_z(0,0,z)\right]dz \\ &\qquad = -j\omega\mu_0 \int_0^b \int_z^{z+\Delta z} H_y(x,0,z)\,dx\,dz \end{aligned} \tag{4}$$

The field quantities in (4) are the total fields. Since $b << \lambda$, the total line-to-line voltage can be defined in the quasi-static sense as

$$V(z) = -\int_0^b E_x(x,0,z)\,dx \tag{5}$$

On the perfectly conducting wires, the total tangential electric fields $E_z(b,0,z)$ and $E_z(0,0,z)$ must be zero. Dividing (4) by Δz and taking the limit as Δz approaches zero gives the following differential equation

$$\frac{dV(z)}{dz} = j\omega\mu_0 \int_0^b H_y(x,0,z)\,dx = j\omega\mu_0 \int_0^b H_y^{\text{inc}}(x,0,z)\,dx + j\omega\mu_0 \int_0^b H_y^{\text{sca}}(x,0,z)\,dx \tag{6}$$

where we have decomposed the total magnetic field in incident and scattering components. The last integral in (6) represents the magnetic flux produced by the current $I(z)$ flowing in each conductor. According to the assumptions (a) and (b) of the STL model, the magnetic flux density produced by this current can be calculated using Biot-Savart's law and the result is

$$\Phi(z) = -\mu_0 \int_0^b H_y^{\text{sca}}(x,0,z)\,dx = L'I(z) \tag{7}$$

The proportionality constant between $\Phi(z)$ and $I(z)$ is the per-unit-length inductance L' [9] of the transmission line. Inserting the inductance term into (6), we obtain the first generalized telegraph's equation

$$\frac{dV(z)}{dz} + j\omega L'I(z) = j\omega\mu_0 \int_0^b H_y^{\text{inc}}(x,0,z)\,dx \tag{8}$$

To derive the second telegraph's equation, we assume that the medium surrounding the line has permittivity constant $\varepsilon = \varepsilon_r \varepsilon_0$. We start from Maxwell's equation

$$\vec{\nabla} \times \vec{H} = j\omega\varepsilon\vec{E} + \vec{J} \tag{9}$$

For a closed surface S, Stokes' theorem applied to a vector function $\vec{F}$ gives

$$\oiint_S \vec{\nabla} \times \vec{F} \cdot d\vec{S} = 0 \tag{10}$$

Letting $\vec{F}$ represent the $\vec{H}$ field of (9) with the closed surface surrounding one of the conductors as shown in Figure 2, we obtain

$$I(z+\Delta z) - I(z) + j\omega\varepsilon \iint_{S_1} E_r r d\phi dz = 0 \tag{11}$$

where E_r is the total radial electric field in the vicinity of the wire surrounded by the partial cylindrical surface S_1, as shown in Figure 2. The total field can be decomposed into incident and scattered components. Upon dividing by Δz and taking the limits as $r \to a$ and $\Delta z \to 0$, (11) it becomes

$$\frac{dI(z)}{dz} + j\omega\varepsilon \int_0^{2\pi} E_r^{\text{sca}} a d\phi + j\omega\varepsilon \int_0^{2\pi} E_r^{\text{inc}} a d\phi = 0 \tag{12}$$

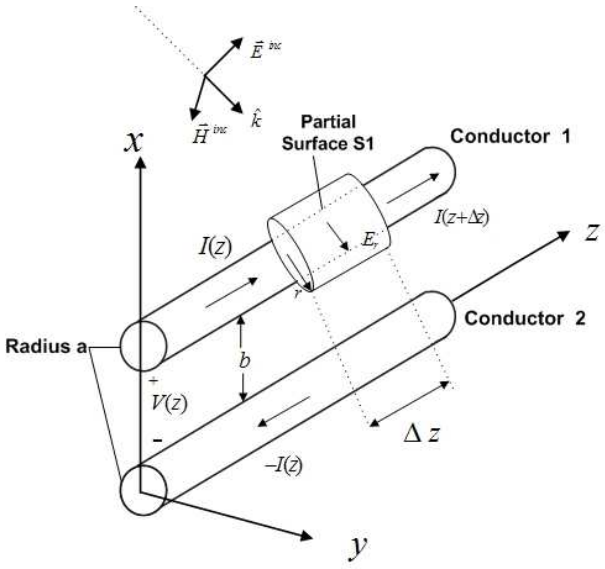

FIGURE 2. Closed surface surrounding one conductor**.**

According to the assumption (a) of the STL model, the electric filed in the vicinity of the line wires can be assumed to be independent of the angle ϕ around the wire. Consequently, the first integral in (12) becomes

$$j\omega\varepsilon\int_0^{2\pi} E_r^{\text{sca}} a\,d\phi = j\omega q'(z) \tag{13}$$

where $q'(z)$ is the linear charge density along conductor. The second integral in (12) involving the incident field is zero because there are no free charges in the vicinity of the wire. Thus, the second telegrapher's equation becomes

$$\frac{dI(z)}{dz} + j\omega q'(z) = 0 \tag{14}$$

We can express this equation in terms of a voltage by introducing a per-unit length capacitance C' [9], which relates the line charge to the scattered component of the line voltage as

$$q'(z) = C'V^{\text{sca}}(z) \tag{15}$$

The total line-to-line voltage is given as

$$V(z) = V^{\text{inc}}(z) + V^{\text{sca}}(z) = -\int_0^b E_x^{\text{inc}}(x,0,z)dx + V^{\text{sca}}(z) \tag{16}$$

Then, (14), (15) and (16) can be combined to give the second telegrapher's equation

$$\frac{dI(z)}{dz} + j\omega C'V(z) = -j\omega C'\int_0^b E_x^{\text{inc}}(x,0,z)dx \tag{17}$$

To obtain a unique solution for the equations (8) and (17), it is necessary to include appropriate boundary conditions relating $V(z)$ and $I(z)$ at the ends of the line. For a finite line of length s, which is terminated in load impedances Z_1 and Z_2 as shown in Figure 3, the following relationships must be included for a unique solution

$$V(0) = -Z_1 I(0),\ V(s) = \mathrm{Z}_2 I(s) \tag{18}$$

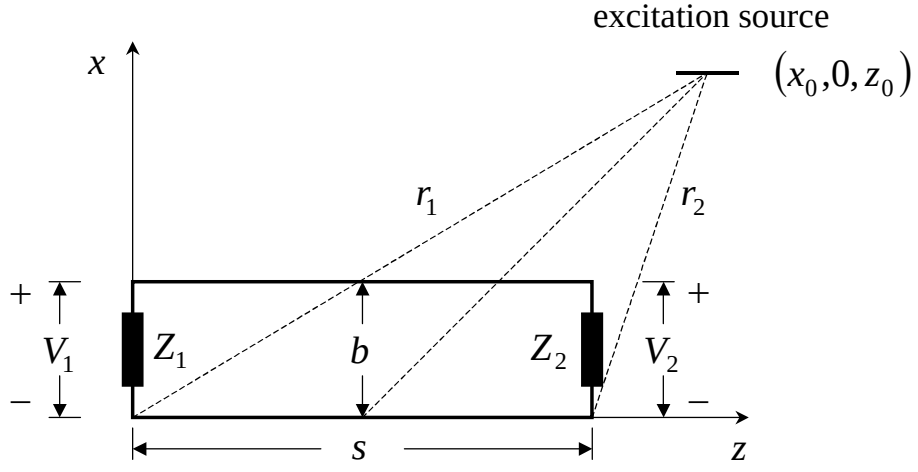

FIGURE 2. Terminated two-wire transmission line.

Note that the negative sign in the first end condition (18) arises from the definition of positive current flow. The coupled equations (8) and (17) can be solved analytically using a chain matrix approach. The result is [7, 8]

$$V_1 = \frac{Z_1}{D}\left\{-\int_0^s K(z)\left[Z_c \cosh\gamma(z-s) - Z_2 \sinh\gamma(z-s)\right]dz \right. \\ \left. + Z_c\int_0^b E_x^{\text{inc}}(x,0,s)dx - \left(Z_c \cosh\gamma s + Z_2 \sinh\gamma s\right)\int_0^b E_x^{\text{inc}}(x,0,0)dx\right\} \tag{19}$$

$$V_2 = \frac{Z_2}{D}\left\{\int_0^s K(z)\left(Z_c \cosh\gamma z + Z_1 \sinh\gamma z\right)dz \right. \\ \left. - \left(Z_c \cosh\gamma s + Z_1 \sinh\gamma s\right)\int_0^b E_x^{\text{inc}}(x,0,s)dx + Z_c\int_0^b E_x^{\text{inc}}(x,0,0)dx\right\} \tag{20}$$

where $K(z) = E_z^{\text{inc}}(b,0,z) - E_z^{\text{inc}}(0,0,z)$, $D = (Z_1 + Z_2)Z_c \cosh\gamma s + \left(Z_1 Z_2 + Z_c^2\right)\sinh\gamma s$ and γ is the complex propagation constant of the transmission line. In cases of a lossless transmission line in free space, the propagation constant is $\gamma = jk$, where $k = 2\pi/\lambda$. With Z_c we denote the characteristic impedance of the transmission line. For the lossless case, this is given by $Z_c = L'/C'$.

TRANSMISSION LINE EXCITATION BY NONUNIFORM FIELDS

In evaluating the response of transmission lines to external fields, it is customary to assume that the incident field is a plane wave. The plane wave can approximate the local behavior of actual fields in the far-field region of realizable emitters. However, this approximation is valid only when studying interactions with objects or devices that are electrically small within the frequency range of the incidents fields. Under high-frequency excitation, it is highly likely that operating transmission lines are electrically long within the frequency range of the interfering fields often encountered in practice. On the other hand, only a few studies that take into account no uniformities in the excitation fields can be found in the open literature [7, 8, 10].

Two different nonuniform excitation fields are examined in this work. The field generated by an elementary electric dipole parallel to the line conductors and the field produced by an idealized spherical-wave source. The location of the dipole is taken to be at $(x_0,0,z_0)$ and the far-field components of the excitation field involved in (19) and (20) are given by [11]

$$E_x^{\text{inc}}(x,0,z) = A\frac{(x-x_0)(z-z_0)}{\left[\sqrt{(x-x_0)^2+(z-z_0)^2}\right]^3}e^{-jk\sqrt{(x-x_0)^2+(z-z_0)^2}} \tag{21}$$

$$E_z^{\text{inc}}(x,0,z) = -A\frac{(x-x_0)^2}{\left[\sqrt{(x-x_0)^2+(z-z_0)^2}\right]^3}e^{-jk\sqrt{(x-x_0)^2+(z-z_0)^2}} \tag{22}$$

where A is a constant analogous to the dipole moment. The corresponding expressions for a linearly polarized spherical wave generated by a point source at $(x_0,0,z_0)$ are

$$E_x^{\text{inc}}(x,0,z) = B\frac{z-z_0}{(x-x_0)^2+(z-z_0)^2}e^{-jk\sqrt{(x-x_0)^2+(z-z_0)^2}} \tag{23}$$

$$E_z^{\text{inc}}(x,0,z) = -B\frac{x-x_0}{(x-x_0)^2+(z-z_0)^2}e^{-jk\sqrt{(x-x_0)^2+(z-z_0)^2}} \tag{24}$$

where B is a constant determining the strength of the spherical wave. Note especially that any choice of dipole or source position (x_0, y_0, z_0) with $y_0 \neq 0$ yields weaker excitation fields; therefore, only worst-case scenarios with $y_0 = 0$ are of interest herein.

A plane-wave excitation field is also considered, which may be expressed as

$$E_x^{\text{inc}}(x,0,z) = E_0 \cos\theta_0 e^{-jk(-x\sin\theta_0 + z\cos\theta_0)} \tag{25}$$

$$E_z^{\text{inc}}(x,0,z) = E_0 \sin\theta_0 e^{-jk(-x\sin\theta_0 + z\cos\theta_0)} \tag{26}$$

where θ_0 is the angle between the z axis and the propagation vector $\vec{k} = k(-\hat{x}\sin\theta_0 + \hat{z}\cos\theta_0)$. The overall factor E_0 denotes the complex amplitude of the plane wave.

For the purpose of direct comparison, all three excitation fields considered in this paper are properly normalized (see [12]) so as to be unitary at the center of the lower conductor $(0,0,s/2)$. In any of the three excitation cases, the integrals in (19) and (20) can be evaluated numerically via standard quadrature routines. Approximate closed-form expressions can be obtained for the second and third integrals in (19) and (20) [12].

RESULTS AND CONCLUSIONS

In this section, we present numerical results for the real and imaginary parts of the induced load voltages V_1 and V_2. We assume that the excitation source (dipole or spherical-wave source) is located at $(x_0,0,z_0) = (d,0,d+s/2)$, where d is a distance parameter. The results are for a lossless transmission line with $b/\lambda = 1/20$ and $s/\lambda = 100/3$. The line is terminated in matched loads; that is $Z_1 = Z_2 = Z_c$. The position of the source varies with the parameter d, but the angle between the lower conductor axis and the displacement vector from its center $(0,0,s/2)$ to the source remains unaltered and equal to 45 degrees. The real and imaginary parts of the load voltages V_1 and V_2 for the excitation field of (21) and (22) are shown in Figures 4 and 5, respectively, as functions of d/λ. The horizontal axis in these graphs is in logarithmic scale. As can be seen from Figures 4 and 5, the load responses exhibit rapid variations as d/λ increases from 10 to 100. For larger values of d/λ, the load voltages begin to stabilize slowly and reach their "final" values, which are virtually identical to those occurring for the excitation field of (25) and (26) with $\theta_0 = 3\pi/4$. A similar behavior is observed for the excitation field of (23) and (24) [12]. The relevant plots are not shown here.

Numerous checks have revealed that the oscillating behavior discussed above is representative of what should be expected for typical nonuniform excitation fields and not very short transmission lines. For a fixed position of the excitation source, the spatial frequency of these oscillations decays as s decreases with b unaltered. The oscillations finally disappear, but the load voltages may still deviate significantly from those predicted under the assumption of plane-wave incidence. As an example, results for a line with $s/\lambda = 10/3$ are depicted in Figure 6. All other parameters are the same as above. For brevity, only the left-end load voltage V_1 is shown. As can be seen, both the real and imaginary parts of V_1 still exhibit an evident dependence on d/λ.

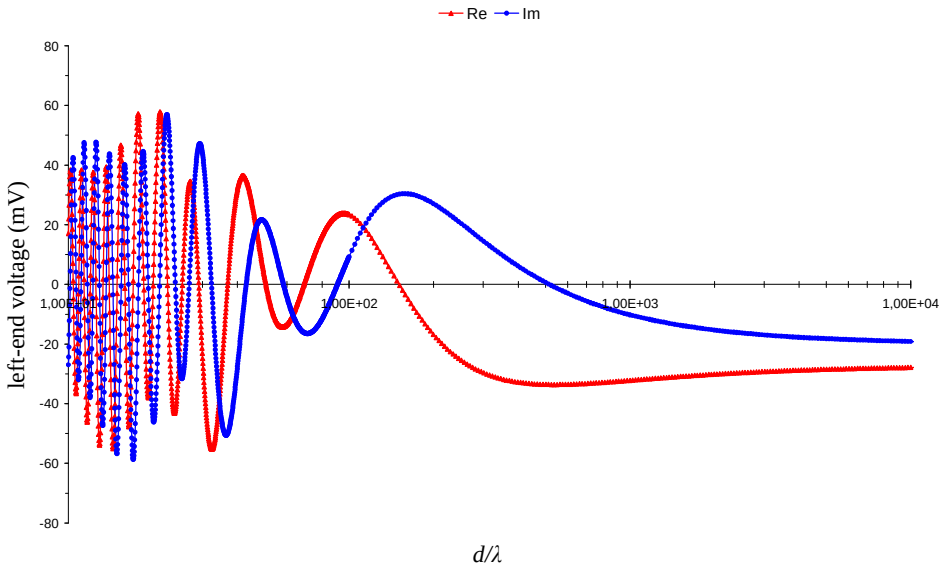

FIGURE 4. Plot of the load voltage V_1 as function of d/λ for the field generated by an elementary dipole and a transmission line with $b/\lambda = 1/20$ and $s/\lambda = 100/3$.

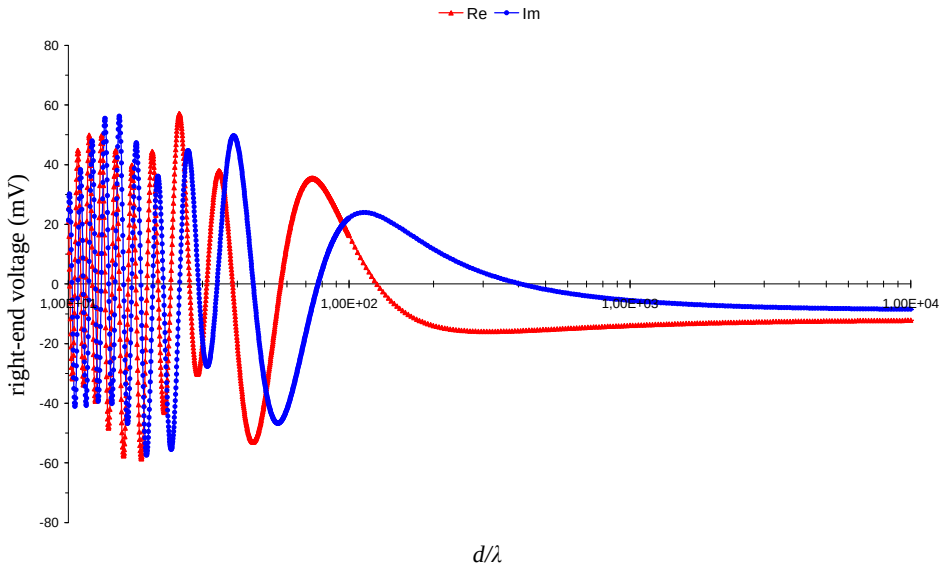

FIGURE 5. Plot of the load voltage V_2 as function of d/λ for the field generated by an elementary dipole and a transmission line with $b/\lambda = 1/20$ and $s/\lambda = 100/3$.

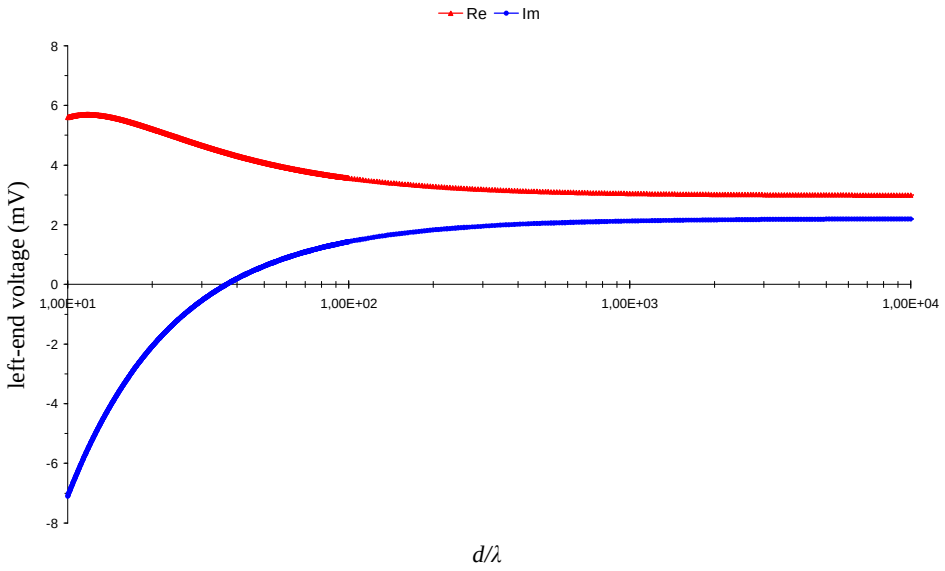

FIGURE 6. Plot of the load voltage V_1 as function of d/λ for the field generated by an elementary dipole and a transmission line with $b/\lambda = 1/20$ and $s/\lambda = 10/3$.

Numerical results presented here manifest that the load response of a two-wire transmission line excited by a nonuniform EM field may differ significantly from that excited by a plane wave arriving from the same direction. The discrepancies become more pronounced for electrically longer lines, a fact that is particularly important in view of the increasing use of microwave frequencies in numerous contemporary applications.

ACKNOWLEDGMENT

The authors would like to thank Lt. Commander of Hellenic Navy D. Filinis for his help and encouragement during the preparation of this paper.

REFERENCES

1. R. F. Harrington, *Field Computation by Moments Methods*, IEEE Press, 1993.
2. F. M. Tesche, M. V. Ianoz, and T. Karlsson, *EMC Analysis Methods and Computational Models*, Wiley, 1997.
3. C. R. Paul, *Analysis of Multiconductor Transmission Lines*, Wiley, 1994.
4. S. Tkatchenko, F. Rachidi, and M. Ianoz, "Electromagnetic filed coupling to a line of finite length: Theory and fast iterative solution in frenquency and time domains," *IEEE Trans. Electromagn. Compat.*, **37,** 509-518 (1995).
5. S. Tkatchenko, F. Rachidi, and M. Ianoz, "High-frequency electromagnetic field coupling to long terminated wires," *IEEE Trans. Electromagn. Compat.*, **43,** 117-129 (2001).

6. T. J. Cui, W. C. Chew, “A full-wave model of wire structure with arbitrary cross sections,” *IEEE Trans. Electromagn. Compat.*, **45,** 626-635 (2003).
7. C. D. Taylor, R. S. Satterwhite, and C. W. Harrison, “The response of a terminated two-wire transmission line excited by a nonuniform electromagnetic field,” *IEEE Trans. Antennas Propagat.*, **13**, 987-989 (1965).
8. A. A. Smith, “A more convenient form of the equations for the response of a transmission line excited by nonuniform fields,” *IEEE Trans. Electromagn. Compat.*, **15**, 151-152 (1973).
9. D. M. Pozar, *Microwave Engineering*, Wiley, 1998.
10. A. A. Smith, “The response of a two-wire transmission line excited by the nonuniform electromagnetic fields of a nearby loop,” *IEEE Trans. Electromagn. Compat.*, **16**, 196-200 (1974).
11. C. A. Balanis, *Antenna Theory*, Wiley, 2005.
12. P. J. Papakanellos and G. V. Veropoulos, “On the load response of terminated transmission lines exposed to external electromagnetic fields,” *IET Microw. Antennas Propagat.*, to be published.